PCP
PLANT & CELL PHYSIOLOGY

Altered Plant and Nodule Development and Protein *S*-Nitrosylation in *Lotus japonicus* Mutants Deficient in *S*-Nitrosoglutathione Reductases

Manuel A. Matamoros[1,*], Maria C. Cutrona[1], Stefanie Wienkoop[2], Juan C. Begara-Morales[3], Niels Sandal[4], Irene Orera[5], Juan B. Barroso[3], Jens Stougaard[4] and Manuel Becana[1]

[1]Departamento de Nutrición Vegetal, Estación Experimental de Aula Dei, Consejo Superior de Investigaciones Científicas, Apartado 13034, 50080 Zaragoza, Spain
[2]Division of Molecular Systems Biology, Department of Ecogenomics and Systems Biology, University of Vienna, Vienna 1090, Austria
[3]Group of Biochemistry and Cell Signaling in Nitric Oxide, Department of Experimental Biology, Faculty of Experimental Sciences, Center for Advanced Studies in Olive Grove and Olive Oils, Campus Universitario "Las Lagunillas", University of Jaén, 23071 Jaén, Spain
[4]Department of Molecular Biology and Genetics, Centre for Carbohydrate Recognition and Signalling, Aarhus University, Gustav Wieds Vej 10, 8000 Aarhus C, Denmark
[5]Proteomics Unit, Centro Investigaciones Biomédicas de Aragón, Instituto Aragonés de Ciencias de la Salud, 50059 Zaragoza, Spain
*Corresponding author: E-mail, m.matamoros@csic.es; Fax, +34-976-716145.
(Received July 18, 2019; Accepted September 8, 2019)

Nitric oxide (NO) is a crucial signaling molecule that conveys its bioactivity mainly through protein *S*-nitrosylation. This is a reversible post-translational modification (PTM) that may affect protein function. *S*-nitrosoglutathione (GSNO) is a cellular NO reservoir and NO donor in protein *S*-nitrosylation. The enzyme *S*-nitrosoglutathione reductase (GSNOR) degrades GSNO, thereby regulating indirectly signaling cascades associated with this PTM. Here, the two GSNORs of the legume *Lotus japonicus*, LjGSNOR1 and LjGSNOR2, have been functionally characterized. The *LjGSNOR1* gene is very active in leaves and roots, whereas *LjGSNOR2* is highly expressed in nodules. The enzyme activities are regulated in vitro by redox-based PTMs. Reducing conditions and hydrogen sulfide-mediated cysteine persulfidation induced both activities, whereas cysteine oxidation or glutathionylation inhibited them. *Ljgsnor1* knockout mutants contained higher levels of *S*-nitrosothiols. Affinity chromatography and subsequent shotgun proteomics allowed us to identify 19 proteins that are differentially *S*-nitrosylated in the mutant and the wild-type. These include proteins involved in biotic stress, protein degradation, antioxidant protection and photosynthesis. We propose that, in the mutant plants, deregulated protein *S*-nitrosylation contributes to developmental alterations, such as growth inhibition, impaired nodulation and delayed flowering and fruiting. Our results highlight the importance of GSNOR function in legume biology.

Keywords: Legume nodules • Nitrosothiols • *S*-nitrosoglutathione • *S*-nitrosoglutathione reductase • *S*-nitrosylation.

Introduction

Nitric oxide (NO) is a gaseous free radical that plays a crucial signaling and regulatory role in plant and animal development (Hirst and Robson 2011, Domingos et al. 2015). It can directly bind [Fe-S] clusters and heme Fe, but also performs biological functions through *S*-nitrosylation of cysteine residues of proteins. This is a reversible post-translational modification (PTM) that may affect protein activity and subcellular localization (Kovacs and Lindermayr 2013). *S*-nitrosoglutathione (GSNO) is formed by the spontaneous and reversible reaction of reduced glutathione (GSH; γGlu-Cys-Gly) with NO (Kovacs and Lindermayr 2013). GSNO is a relatively stable NO reservoir and, as a major physiological NO donor, participates in protein *S*-nitrosylation. The enzyme *S*-nitrosoglutathione reductase (GSNOR) is highly conserved in all organisms because it regulates the cellular homeostasis of *S*-nitrosothiols (SNOs), of which GSNO is the most abundant (Feechan et al. 2005, Corpas et al. 2013, Lindermayr 2018). GSNOR belongs to the class III alcohol dehydrogenase family and was initially characterized in *Arabidopsis thaliana* as a GSH-dependent formaldehyde dehydrogenase (Martínez et al. 1996). It was subsequently demonstrated that the enzymes from bacteria, yeast, mammals and plants are highly specific for GSNO and that their main function is the regulation of intracellular SNO levels (Jensen et al. 1998, Liu et al. 2001, Sakamoto et al. 2002). GSNOR determines the equilibrium between *S*-nitrosylated proteins and GSNO and may therefore regulate indirectly signaling cascades associated with protein *S*-nitrosylation.

Recent research underlines an important role of GSNOR in plant biology. Studies with overexpressing and knockout mutants of *A. thaliana* suggest that GSNOR regulates multiple genetic networks integral to plant development (Kwon et al. 2012). In tomato (*Solanum lycopersicum*), reduction of GSNOR expression by RNAi affects fruit formation and seed germination (Hussain et al. 2019). Moreover, GSNOR also plays a role in the defense of plants against pathogens (Feechan et al. 2005, Rustérucci et al. 2007, Hussain et al. 2019) and in their

Plant Cell Physiol. 61(1): 105–117 (2020) doi:10.1093/pcp/pcz182, Advance Access publication on 16 September 2019, available online at https://academic.oup.com/pcp

response to abiotic stress conditions, including low or high temperatures and mechanical injury (Díaz et al. 2003, Corpas et al. 2013, Kubienová et al. 2014). The alterations observed in *Atgsnor* null mutants in growth, development and stress responses may be due, at least in part, to the modification of salicylic acid- and auxin-dependent signaling networks (Díaz et al. 2003, Feechan et al. 2005, Shi et al. 2015).

Most legumes have the ability to establish symbiotic associations with rhizobia leading to the formation of root nodules. These unique organs provide optimal conditions for the expression of bacterial nitrogenase whose activity supplies fixed nitrogen to the plants in exchange of photosynthetically-derived sugars (Udvardi and Poole 2013). NO has important signaling roles in nitrogen-fixing and mycorrhizal symbioses (Frendo et al. 2013, Martínez-Medina et al. 2019). However, nothing is known about the presence of GSNOR in nodules. This is somewhat surprising because there are substantial commonalities between symbiotic and pathogenic systems (Gourion et al. 2015) and also because GSNOR plays a relevant role during pathogen attack and in the subsequent plant's defense response (Feechan et al. 2005). Genetic and molecular studies of the legume-rhizobia symbiosis are greatly facilitated by using *Medicago truncatula* or *Lotus japonicus* as model plants for indeterminate or determinate nodulation, respectively. Large mutant collections exist for both species and their genomes have been fully sequenced (Sato et al. 2008, Tang et al. 2014). In this work, *L. japonicus* was selected because it was previously used to characterize the pathway for the synthesis of GSH and its legume-specific homolog homoglutathione (hGSH; γGlu-Cys-βAla; Matamoros et al. 2003). The two GSNOR enzymes, LjGSNOR1 and LjGSNOR2, have been functionally characterized by producing the recombinant enzymes and by phenotyping gene-specific mutants. Our results indicate that SNO homeostasis by means of GSNOR activity is essential for proper development of legume plants and nodules.

Results and Discussion

The *Lotus japonicus* genome encodes two functional GSNORs

The *GSNOR* gene is predominantly found as single-copy in most species analyzed so far, including *A. thaliana* (At5g43940). However, poplar (*Populus trichocarpa*), diploid cotton (*Gossypium raimondii*) and the moss *Physcomitrella patens* are predicted to have two gene copies (Xu et al. 2013). Legumes such as soybean (*Glycine max*), common bean (*Phaseolus vulgaris*) and *M. truncatula* also contain two *GSNOR* copies, although it is uncertain whether both code for active proteins. In our study, two genes of *L. japonicus*, *LjGSNOR1* and *LjGSNOR2*, have been identified and fully characterized at the physiological, biochemical and molecular levels. They encode, respectively, proteins of 380 and 379 amino acids that share ∼92% identity and are ∼90% identical to the *A. thaliana* GSNOR (AtGSNOR). The amino acid residues that participate in substrate binding in AtGSNOR (Xu et al. 2013, Lindermayr 2018) and in tomato GSNOR (Kubienová et al. 2013) are well conserved in *L. japonicus* and other legume homolog enzymes (**Supplementary Fig. S1**). LjGSNOR1 and LjGSNOR2 contain 13 and 15 Cys residues, respectively, that are highly conserved. Two of them (Cys47 and Cys177, based on LjGSNOR2 numbering) coordinate catalytic Zn^{2+}, whereas Cys99, Cys102, Cys105 and Cys113 coordinate structural Zn^{2+}. Only two Cys residues are not conserved between LjGSNOR1 and LjGSNOR2: Cys285, replaced by Thr in LjGSNOR1 and *M. truncatula* GSNOR1, and Cys373, replaced by Val in LjGSNOR1 and tomato GSNOR (**Supplementary Fig. S1**). Because Cys residues may be a target of reactive oxygen species and NO-dependent PTMs (Waszczak et al. 2015), they could be important for the differential regulation of LjGSNOR1 and LjGSNOR2.

Besides structural factors, protein localization determines the interactions with other proteins, post-translational regulation and participation in signaling networks. To ascertain the possible functional diversification of LjGSNOR1 and LjGSNOR2, we analyzed the theoretical subcellular localization of the proteins and the expression profiles of the genes in several plant organs. Most plant GSNORs are predicted to be cytosolic (Xu et al. 2013). Consistent with this, subcellular prediction programs (ChloroP, Mitoprot, Predotar, PTS1, PSORT and TargetP) did not provide an extra-cytosolic localization of the *L. japonicus* enzymes.

Transcriptional evidence for the expression of the two *LjGSNOR* genes was initially obtained from the *L. japonicus* Expression Atlas (Mun et al. 2016). Array data indicate that *LjGSNOR1* expression is up-regulated in pods and seeds, whereas *LjGSNOR2* is highly expressed in nodules. The mRNA levels of *LjGSNOR2* were modest in the pods and seeds and very low in the rest of the plant. These data were validated by quantitative reverse transcription-polymerase chain reaction (qRT-PCR) using specific primers for *LjGSNOR1* and *LjGSNOR2* (**Fig. 1**). This analysis confirmed that *LjGSNOR1* is highly expressed in seeds, especially in the embryo, and strongly suggested that *LjGSNOR2* is a nodulin due to its enhanced expression levels in nodules relative to leaves or roots; however, this gene was up-regulated also in the embryo and pollen (**Fig. 1**). The expression profile of *LjGSNOR2* contrasts with that of *AtGSNOR*, which is highly expressed in most plant organs, except in mature pollen (Winter et al. 2007), and with tomato *GSNOR*, which is strongly up-regulated in the pistil and stamens and in ripening fruits (Kubienová et al. 2013). The expression profiles of *LjGSNOR* genes strongly suggest an important role of both gene products in seed development and germination, as well as specific functions of LjGSNOR2 in symbiotic nitrogen fixation.

LjGSNOR1 and LjGSNOR2 kinetic parameters

GSH is a major water soluble antioxidant and redox buffer in most organisms (Noctor et al. 2012). In many legume species and tissues, hGSH partially or completely replace GSH (Frendo et al. 1999, Matamoros et al. 1999). That is the case of *L. japonicus*, which produces exclusively hGSH in leaves and roots and the two thiols in nodules. However, in nodules GSH is probably generated by the bacteroids (Matamoros et al. 2003). Thus, *S*-nitrosohomoglutathione (hGSNO) rather than GSNO is

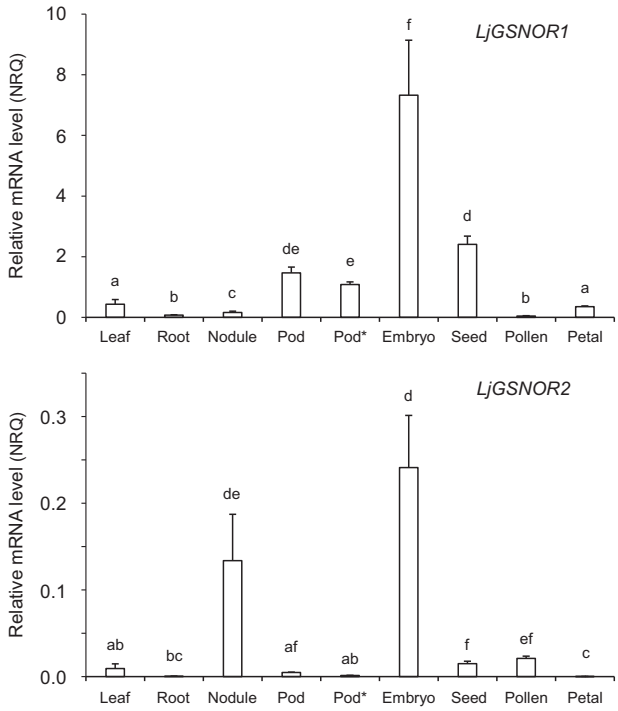

Fig. 1 Expression profiles of *LjGSNOR1* and *LjGSNOR2* in plant organs. Transcript levels were determined by qRT-PCR. Pod* denotes seedless pods. Normalized relative quantification (NRQ) values were obtained using *ubiquitin* and *ATP synthase* as reference genes. Data are means ± SE of 3–4 biological replicates. Statistical analyses were performed using $\log_2$(1/NRQ)-transformed data (Rieu and Powers 2009). Means denoted by the same letter are not significantly different at *P*-value <0.05 based on the Duncan's multiple range test.

expected to be present in *L. japonicus* non-symbiotic tissues. To investigate whether LjGSNOR1 and LjGSNOR2 possess differential affinities for GSNO and hGSNO, both proteins were overproduced in *Escherichia coli*, purified to homogeneity and characterized (**Supplementary Fig. S2**). In addition, the dehydrogenase activities of both enzymes were determined using *S*-(hydroxymethyl)glutathione (HMGSH) as a substrate. Kinetic parameters were calculated using nonlinear regression analyses. Our results showed that LjGSNOR1 and LjGSNOR2 catalyze NADH-dependent reduction of GSNO and hGSNO at similar rates (**Table 1**). Both enzymes were slightly more efficient in reducing GSNO than hGSNO, suggesting that the presence of hGSNO in legumes does not imply the existence of a specific hGSNO reductase. Similarly to the results reported by Kubienová et al. (2013), LjGSNOR1 and LjGSNOR2 showed higher reaction rates and catalytic efficiencies with GSNO than with HMGSH, indicating that the in vivo function of both proteins is mainly related to the regulation of (h)GSNO and hence of protein *S*-nitrosylation levels.

LjGSNOR1 and LjGSNOR2 are subjected to post-translational regulation

Protein PTM constitutes a fast and versatile way to modulate their function. In this regard, *S*-nitrosylation, glutathionylation and other redox-based PTMs are emerging as central factors in protein regulation (Zaffagnini et al. 2012, Kovacs and Lindermayr 2013, Waszczak et al. 2015). GSNORs contain numerous highly conserved Cys residues (**Supplementary Fig. S1**; Xu et al. 2013) that may be sensitive to redox changes. Thus, we investigated the effects of oxidants, reductants and signal molecules on LjGSNOR1 and LjGSNOR2 activities (**Fig. 2**). The two recombinant proteins were sharply affected by oxidation. Incubation with 5 mM hydrogen peroxide (H_2O_2) caused a ~90% decrease of activity. Similarly, the H_2O_2 treatment of AtGSNOR induced the oxidation of the two residues (Cys47 and Cys177) that coordinate catalytic Zn^{2+} and, indeed, the subsequent loss of enzyme activity has been attributed to release of Zn^{2+} (Kovacs et al. 2016). On the contrary, reducing agents such as dithiothreitol (DTT) and β-mercaptoethanol caused slight but significant increases, suggesting that the complete reduction of certain Cys residues is necessary to achieve maximal activities. These results appear to be at odds with those reported by Kubienová et al. (2013) for tomato GSNOR, which was inhibited by DTT, β-mercaptoethanol or ascorbic acid. In contrast, DTT restored AtGSNOR activity after inhibition by H_2O_2, paraquat and *S*-nitrosylation (Guerra et al. 2016, Kovacs et al. 2016). Our study of *S*-nitrosylation of *L. japonicus* enzymes produced unexpected results. LjGSNOR1 activity remained unaffected by treatment with 1 mM GSNO (molar ratio of GSNO to protein ~80), but declined by 60% when the concentration of GSNO was raised to 5 mM (molar ratio ~400) (**Fig. 2**). This indicated that, at least under our experimental conditions, LjGSNOR1 is less susceptible to inhibition by *S*-nitrosylation than is AtGSNOR (Guerra et al. 2016). Regarding LjGSNOR2, the activity was not affected by treatment with 1–5 mM GSNO (**Fig. 2**). The biotin-switch assay indicated that both LjGSNOR1 and LjGSNOR2 are *S*-nitrosylated after treatment with 1 mM GSNO (**Supplementary Fig. S3**). These results suggest that the modification of more than one reactive Cys residue in LjGSNOR1 is required for down-regulation of enzyme activity, whereas *S*-nitrosylation of LjGSNOR2 does not necessarily entail protein inhibition. Although the concentration of (h)GSNO in *L. japonicus* remains to be elucidated, *S*-nitrosylation could inhibit LjGSNOR1 activity in the leaves, especially under high NO generating conditions such as pathogen attack or abiotic stress (Umbreen et al. 2018). This would enhance protein *S*-nitrosylation and amplify the NO signal. The reasons for the different susceptibility of LjGSNOR1

Table 1 Kinetic parameters of LjGSNOR1 and LjGSNOR2

Enzyme	Substrate	V_{max} (μmol min^{-1} mg^{-1})	K_m (μM)	V_{max}/K_m
LjGSNOR1	GSNO	12.03 ± 0.16	20.2 ± 1.25	0.60
	hGSNO	13.03 ± 0.67	68.3 ± 4.17	0.19
	HMGSH	0.25 ± 0.021	55.8 ± 4.54	0.0045
LjGSNOR2	GSNO	55.4 ± 1.42	137.8 ± 5.92	0.40
	hGSNO	50.6 ± 3.025	387.9 ± 60.8	0.13
	HMGSH	2.03 ± 0.10	314.3 ± 23.3	0.0065

V_{max} and K_m were calculated using activity values obtained from three independent experiments. Values are means ± SE of three replicates.

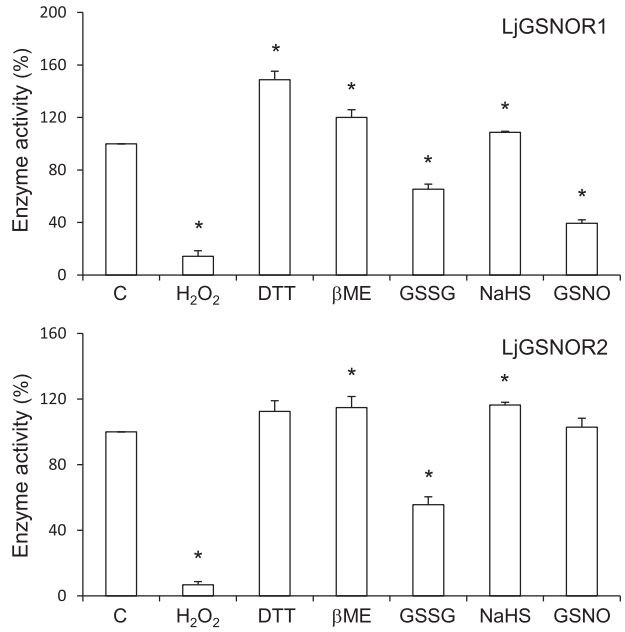

Fig. 2 Effect of several redox-based PTMs on LjGSNOR1 and LjGSNOR2 enzyme activities. Recombinant proteins were treated with 5 mM of H_2O_2, DTT, β-mercaptoetanol (β-ME), NaHS or GSNO for 1 h at 30°C. Controls were incubated with 25 mM Tris–HCl (pH 8.0), except the control of the NaHS treatment, which was supplemented with 5 mM of NaH_2PO_4. For glutathionylation assays, samples were incubated with 25 mM Tris–HCl (pH 8.0) buffer alone (control) or supplemented with 5 mM GSSG, for 5 h at 30°C. Values are means ± SE of 3–6 replicates. Means marked with an asterisk differ significantly from control at *P*-value <0.05 based on the Student's *t*-test. Activity is expressed as percentage relative to each control treatment.

and LjGSNOR2 to *S*-nitrosylation remain obscure. The 13 Cys residues present in LjGSNOR1 are conserved in LjGSNOR2, which contains two additional Cys residues (**Supplementary Fig. S1**). Minor structural differences between the two proteins might explain their differential susceptibility to this PTM, but the possible physiological implications await elucidation.

Next, we investigated if glutathionylation may play a role in the regulation of LjGSNOR1 and LjGSNOR2. This redox-sensitive and reversible PTM involves formation of mixed disulfides between glutathione and reactive Cys residues (Zaffagnini et al. 2012), and may modulate protein activity and confer protection against irreversible inactivation under oxidative conditions. However, nothing is known about the effect of glutathionylation on plant GSNORs. Recombinant LjGSNOR1 and LjGSNOR2 were incubated with different concentrations of glutathione disulfide (GSSG) as glutathionylation agent. Relatively high GSSG concentrations and long incubations times, in accordance with other glutathionylation protocols (Michelet et al. 2005, Melchers et al. 2007), were necessary to achieve significant variations in enzyme activities. Treatment with 5 mM GSSG for 5 h caused a ~40% decrease in enzyme activities (**Fig. 2**). To confirm that LjGSNOR proteins undergo glutathionylation, recombinant LjGSNOR1 and LjGSNOR2 were incubated with 5 mM GSSG and analyzed using matrix-assisted laser desorption/ionization time-of-flight mass spectrometry (MALDI-TOF MS). After treatment, the increases of molecular mass of LjGSNOR1 were variable in different experiments, although in general compatible with the addition of one to three molecules of glutathione per protein (data not shown). For LjGSNOR2, the spectra were more precise and revealed the appearance of a new peak with an increase of ~1,227 Da in its molecular mass (**Fig. 3**). This shift is consistent with the addition of four glutathione molecules per molecule of LjGSNOR2. This high level of glutathionylation is most probably caused by the elevated GSSG concentrations and long incubation times, and might not reflect the in vivo situation. Similarly, high glutathionylation levels have been reported for other proteins. For example, in *A. thaliana* the activity of the glycine decarboxylase complex was inhibited by the *S*-glutathionylation of up to six Cys residues of the P protein (Palmieri et al. 2010). Recently, Zechmann (2014) estimated the glutathione content in different cell compartments from *A. thaliana* leaves. Assuming a GSH:GSSG ratio of 20:1 (Noctor et al. 2012) and optimal conditions, GSSG concentration in the cytosol and mitochondria would be ~0.25 mM and ~0.75 mM, respectively. These concentrations may nevertheless be considerably higher at particular hotspots in cells exposed to oxidative stress. Moreover, GSSG is a product of GSNOR activity and might therefore act as a feedback inhibitor. Low GSSG concentrations could modify only specific Cys residues and cause subtle changes in GSNOR activity compatible with the participation of glutathionylation in redox signaling processes under both physiological and stress conditions. In addition, enzymatically catalyzed *S*-glutathionylation by glutathione *S*-transferases has been observed in animal cells (Zhang et al. 2018). Whether the same mechanism is operative in plants is unknown, but it could greatly increase glutathionylation efficiency at small GSSG concentrations.

Finally, we examined the possible regulation of LjGSNOR1 and LjGSNOR2 by persulfidation of Cys residues (**Fig. 2**). Hydrogen sulfide (H_2S) is emerging as a new signaling molecule that plays important roles in physiological and pathological processes in plants and animals (Aroca et al. 2018). Although H_2S may directly interact with protein metal centers, persulfidation is probably the main mechanism by which this gas transmits its signaling capacity. In this process, a thiol (R-SH) is converted into a perthiol or persulfide (R-SSH), and this may alter protein structure and function because of the decrease in the p*Ka* and the increase in nucleophilicity of the persulfide group (Ono et al. 2014). As far as we know, the post-translational regulation of plant GSNORs by persufidation has not been described. Recombinant proteins were treated with the H_2S donor sodium hydrogen sulfide (NaHS) for 1 h at several concentrations. This treatment significantly increased LjGSNOR1 and LjGSNOR2 activities by 8% and 16%, respectively, indicating that H_2S may act as a regulator of GSNOR. Overall, our results suggest that in plant cells maximal GSNOR activities are achieved under reducing conditions and in the presence of H_2S. Oxidative conditions may indirectly increase *S*-nitrosylation levels through inhibition of GSNOR activity. Likewise, under excessive NO concentrations, GSNOR activity might be inhibited by *S*-nitrosylation and glutationylation, thus amplifying the NO signal.

Characterization of *Ljgsnor* mutants

To investigate the functions of LjGSNOR1 and LjGSNOR2, we used three knockout lines: *Ljgsnor1* 33535; *Ljgsnor1* 60068; and

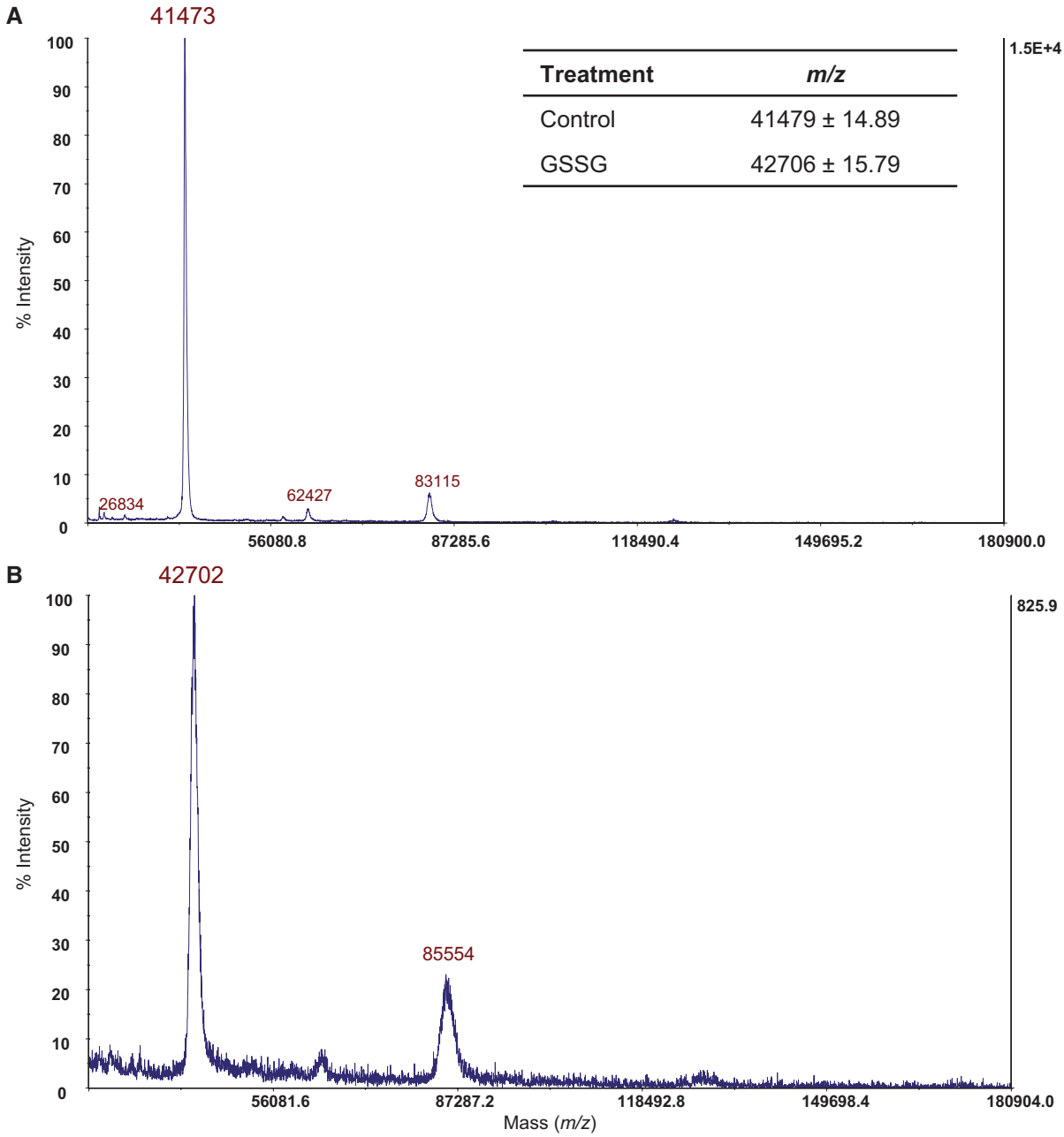

Fig. 3 Glutathionylation of LjGSNOR2. The figure shows MALDI-TOF analyses for (A) the protein incubated in 25 mM Tris–HCl (pH 8.0) and (B) the protein treated with 5 mM GSSG for 5 h at 30°C. The shift in molecular mass reflects the addition of four molecules of glutathione. Values are means ± SE of nine technical replicates.

Ljgsnor2 21012 (see Materials and Methods for further details). First, the degree of silencing of *LjGSNOR1* and *LjGSNOR2* in each line was determined by qRT-PCR. Because *LjGSNOR2* is barely expressed in the leaves (**Fig. 1**; **Supplementary Fig. S4**), *LjGSNOR1* and *LjGSNOR2* mRNA levels were quantified in the leaves and nodules, respectively. Compared with the wild-type (WT), the expression of *LjGSNOR1* in leaves of lines 33535 and 60068 (**Fig. 4A**) and the expression of *LjGSNOR2* in nodules of line 21012 (**Fig. 4B**) were strongly reduced, confirming the validity of the three mutants used in our study. Next, GSNOR activity was determined in the leaves of the *Ljgsnor1* mutants. Both lines exhibited only 15–20% of the GSNOR activity detected in the WT (**Fig. 4C**), confirming that LjGSNOR1 is the major isoform in the leaves. To assess the contribution of LjGSNOR1 to NO homeostasis, the total SNO content of leaves was determined with a Nitric Oxide Analyzer (NOA). Under basal conditions, WT plants had ~85 pmol SNOs mg^{-1} protein. This value is similar to reported SNO concentrations in other plant species using the same detection method (Begara-Morales et al. 2018). *Ljgsnor1* mutant lines contained ~2.5-fold higher SNO levels than the WT (**Fig. 4D**), indicating an important role of LjGSNOR1 in the homeostasis of intracellular SNOs. These results were similar to those obtained with *Atgsnor* mutants (Feechan et al. 2005, Lee et al. 2008) and tomato

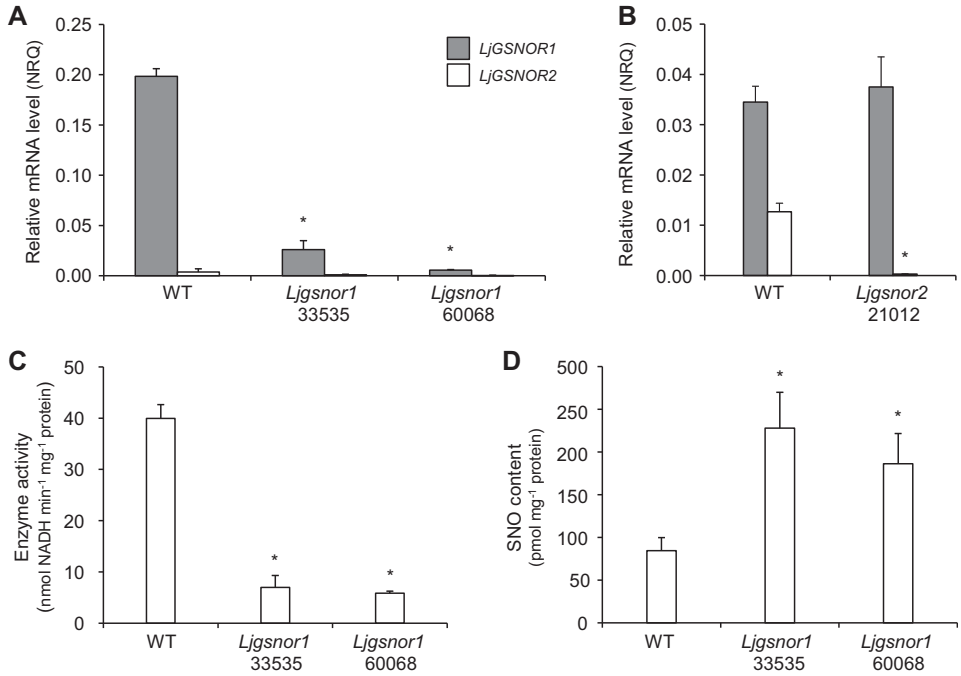

Fig. 4 Characterization of *Ljgsnor* mutants. Transcript levels of *LjGSNOR1* and *LjGSNOR2* were determined by qRT-PCR in leaves (A) and nodules (B) of WT and *Ljgsnor1* and *Ljgsnor2* mutant plants. Normalized relative quantification (NRQ) values were obtained using *ubiquitin* and *ATP synthase* as reference genes. Data are means ± SE of 3–4 biological replicates. Statistical analyses were performed independently for each gene using $\log_2(1/\text{NRQ})$-transformed data. (C) GSNOR activity in the leaves of WT and *Ljgsnor1* mutant plants at 56 d of age. Values are means ± SE of three replicates. Means marked with an asterisk significantly differ from the control at *P*-value <0.05 based on the Student's *t*-test. (D) *S*-nitrosothiol content in leaves of WT and *Ljgsnor1* mutant plants at 56 d of age. Values are means ± SE of four replicates. Means marked with an asterisk significantly differ from the control at *P*-value <0.05 based on the Student's *t*-test.

GSNOR-antisense transgenic lines (Gong et al. 2015). Unfortunately, SNOs could not be determined in nodules of the *Ljgsnor2* mutant due to the relatively high amount of tissue necessary for each biological replicate (~2 g) compared with the amount of nodules produced by mutants (~6 mg per plant). Because thioredoxins can mediate Cys denitrosylation (Benhar et al. 2008) and may potentially compensate for GSNOR deficiency, the transcript profiles of 13 thioredoxin genes of *L. japonicus* (Tovar-Méndez et al. 2011) were determined in the leaves of the WT and the two *Ljgsnor1* mutant lines. However, none of the thioredoxin genes was induced, suggesting that they are not regulated by enhanced SNO levels.

LjGSNOR1 and LjGSNOR2 are involved in plant development

Previous studies showed that *Atgsnor* null mutants were unable to elongate hypocotyls after germination on nutrient medium plates in the dark (Lee et al. 2008). To test if *L. japonicus* mutants have a comparable phenotype, we carried out hypocotyl elongation experiments in the WT and the *Ljgsnor1* and *Ljgsnor2* lines. Seeds were grown in plates for 3 d in the dark, then the plates were placed vertically and the increase in hypocotyl length was measured after three additional days in the dark. The growth of the two *Ljgsnor1* lines was significantly inhibited compared to the WT and *Ljgsnor2* plants (**Fig. 5A**). This observation is in good agreement with the high expression of *LjGSNOR1*, along with the negligible expression of *LjGSNOR2*, in the roots (**Supplementary Fig. S4**). To ascertain that the hypocotyl growth inhibition was caused by enhanced GSNO levels, the changes in hypocotyl elongation were measured in WT seedlings that had been treated or not with 100 μM GSNO. The application of this SNO to seedlings also inhibited hypocotyl elongation, although to a lower extent (compare **Fig. 5A, B**), suggesting that the phenotype of the *Ljgsnor1* mutants was caused, at least in part, by excess GSNO.

Plant and nodule growth was measured at different developmental stages in the WT and mutants. At 28 d of age, the *Ljgsnor1* plants showed significant reductions of plant weight (20–30%), shoot and root length (30–50%) and leaf number (50%) (**Fig. 6**). In sharp contrast, the *Ljgsnor2* mutant plants did not show significant growth alterations, consistent with the negligible expression of the respective gene in leaves and roots. Neither of the *Ljgsnor1* and *Ljgsnor2* mutants showed significant alterations in the nodule number. This strongly suggests that LjGSNOR1 and LjGSNOR2 are not critical for the onset of symbiosis, although LjGSNOR1 is involved in the first stages of plant development, as occurs for AtGSNOR (Kwon et al. 2012, Shi et al. 2015). At 56 d of age the phenotype was somehow more pronounced for the three *Ljgsnor* lines. The *Ljgsnor1* mutants showed reductions of ~70% in the shoot and root weights and of 25–40% in the shoot and root lengths. Moreover, the nodule number and the total weight of nodules decreased by 60% and 80%, respectively (**Fig. 7**). Therefore, the inactivation of *LjGSNOR1* does not affect the initial stages of symbiosis but

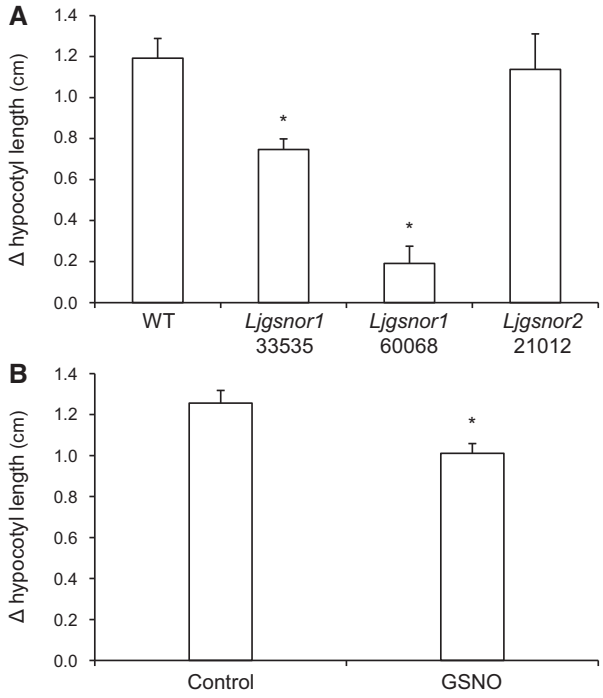

Fig. 5 Hypocotyl elongation of WT, *Ljgsnor1* and *Ljgsnor2* mutant seedlings. (A) After germination, seedlings were grown on plates in the dark for 3 d and the increments of hypocotyl length were measured. (B) WT seedlings were incubated with 50 mM sodium phosphate buffer (pH 7.4) alone (control) or supplemented with 100 μM GSNO. They were then grown on plates in the dark for 3 d and the increments of hypocotyl length were measured. Values are means ± SE of 12–18 seedlings. Means marked with an asterisk differ significantly from the control at *P*-value <0.05 based on the Student's *t*-test.

appears to impair nodule growth afterwards. The *Ljgsnor2* mutant showed a similar phenotype, with decreases of ∼50% in shoot and root weights, ∼25% in shoot length and ∼60% in nodule weight (**Fig. 7**). These observations are puzzling and suggest that LjGSNOR2, although expressed at very low levels in roots and leaves, does affect the development of mature plants.

To rule out the possibility that the general decline in growth of *Ljgsnor1* and *Ljgsnor2* plants at 56 d was caused by impaired nodulation and consequent nitrogen deficiency, plants fed on 8 mM KNO_3 were phenotyped. Under these non-nodulating conditions, *Ljgsnor1* plants showed decreases of 45–60% in shoot and root weights, and the same occurred for the shoot weight of *Ljgsnor2* plants (**Supplementary Fig. S5**). These results suggest that the accumulation of SNOs impacts on plant growth and development irrespective of the nitrogen source. Inactivation of *LjGSNOR1* or *LjGSNOR2* also caused a delay in flowering and fruiting. This observation is interesting because the *Atgsnor1–3* mutant has precocious flowering (Kwon et al. 2012), which may reflect interspecific differences in the effect of high SNO levels on the flowering time. Under our growth conditions, *L. japonicus* WT plants blossomed, on average, 12 weeks after germination, whereas none of the mutant lines had flowered by then (**Fig. 8A**). The *Ljgsnor1* 60068 plants contained on average ∼2 flowers per plant at week 13, whereas the *Ljgsnor1* 33535 and *Ljgsnor2* plants did not flower until weeks 14 or 15. The mutant plants also showed delayed pod emergence and reduced pod yield. In WT plants, pods were visible at week 13 (**Fig. 8B**) and their number increased steadily until week 17, when on average every plant contained ∼18 pods. However, in the mutants, pods were not visible until week 15 and by week 17 all mutant lines contained fewer pods per plant than the WT (**Fig. 8B**).

Ljgsnor1 mutants contain higher levels of endogenously *S*-nitrosylated proteins

Protein *S*-nitrosylation is a major mechanism in NO signaling (Kovacs and Lindermayr 2013). *Ljgsnor1* mutants contain increased levels of SNOs (**Fig. 4D**) and, hence, presumably of *S*-nitrosylated proteins. Because deregulation of protein *S*-nitrosylation might explain some of the observed phenotypic differences between the WT and the mutants, the biotin-switch method (Jaffrey et al. 2001) was used to identify proteins that are differentially *S*-nitrosylated in the leaves of WT and the *Ljgsnor1* mutants. After specific labeling of *S*-nitrosylated Cys residues with biotin, tagged proteins were purified by streptavidin-affinity chromatography. The process included extensive washing to avoid non-specific protein binding and a final elution step with 100 mM DTT. After digestion, the proteins were identified by MS. The *Ljgsnor2* line was not investigated at this point because LjGSNOR2 is hardly expressed in the leaves (**Supplementary Fig. S4**).

Because of the low quantity and lability of the -SNO bond, the identification of endogenously *S*-nitrosylated proteins is a complex and technically challenging process. Consequently, the identified proteins in the different biological replicates showed only a moderate overlap. We performed two independent analyses with a total of five biological replicates per line. In all cases, the amount of *S*-nitrosylated proteins was <1% of total protein. The *S*-nitrosylation sites were examined using the GPS-SNO 1.0 software (Xue et al. 2010), which predicted that 74% of the identified proteins contain one or several *S*-nitrosylation sites (**Supplementary Dataset**) and thus confirmed the reliability of our identifications. In total, 281 proteins were identified. Of these, 8 proteins were detected only in the WT, 16 proteins in *Ljgsnor1* 33535 and 132 proteins in *Ljgsnor1* 60068. There were 72 proteins common to the WT and the mutant lines, which may be ascribed to constitutively *S*-nitrosylated proteins of leaves (**Supplementary Dataset**). In this group, a large number of proteins are related to photosynthesis, which agrees with previous studies suggesting that *S*-nitrosylation fulfills an important regulatory role in this process (Hu et al. 2015). Moreover, seven redox related proteins were identified in the WT and mutants, including three peroxiredoxins (PrxIIB, PrxQ and 2CysPrx), two thioredoxins, ascorbate peroxidase and GDP-mannose 3′,5′-epimerase (**Supplementary Dataset**). Peroxiredoxins PrxIIE of *A. thaliana* (Romero-Puertas et al. 2007) and PrxIIF of pea (Camejo et al. 2015) are inhibited by *S*-nitrosylation. On the contrary, ascorbate peroxidase activity is induced by *S*-nitrosylation of a Cys residue located at the ascorbate binding site (Correa-Aragunde et al. 2013, Begara-Morales et al. 2014). The same regulatory mechanisms might

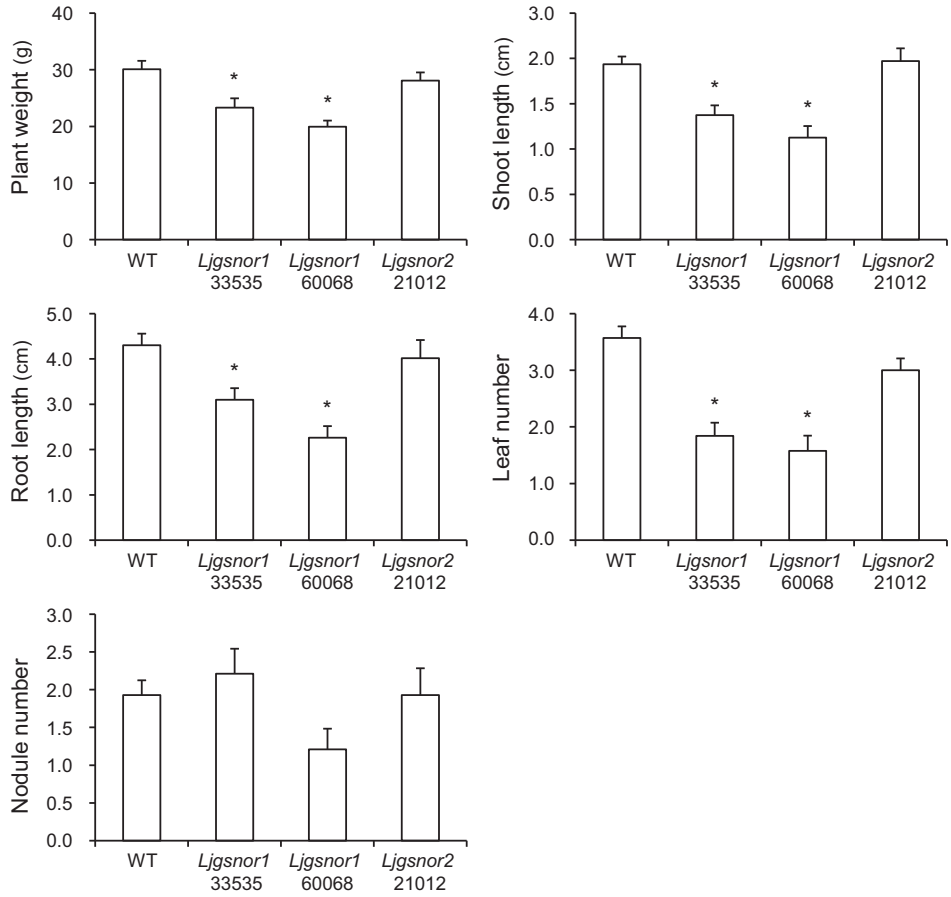

Fig. 6 Phenotypes of WT, *Ljgsnor1* and *Ljgsnor2* plants at 28 d of age. Seedlings were inoculated with *Mesorhizobium loti* strain R7A in plates containing Jensen medium and grown in a controlled-environment chamber. Values are means ± SE of 14–20 plants. Means marked with an asterisk differ significantly from control at *P*-value <0.05 based on the Student's *t*-test. Phenotyping was repeated three times with independently grown sets of plants with similar results.

operate in *L. japonicus* leaves. There is no information on a possible regulatory role of *S*-nitrosylation on ascorbate biosynthesis, but it has been recently shown that an NO-enriched atmosphere increases the ascorbate content of pepper fruits (Rodríguez-Ruiz et al. 2017). The possible implication of the NO-mediated PTM of GDP-mannose 3′,5′-epimerase, a component of the main ascorbate biosynthetic pathway in plants, merits further investigation.

Nineteen proteins were detected in the two independent *Ljgsnor1* mutant lines but not in the WT replicates (**Table 2**). Three of them are involved in the defense response: a class Ia chitinase, a basic secretory protein and a disease resistance response protein. The *S*-nitrosylation of these proteins, along with the increased SNO levels in the *Ljgsnor1* lines (**Fig. 4D**), is fully consistent with the observations that *Atgsnor* null mutants contain increased SNO levels that impair the defense responses and thereby are pathogen sensitive (Feechan et al. 2005, Xu et al. 2013). These authors concluded that deregulated *S*-nitrosylation of resistance proteins might contribute to the alteration of the plant's defense response. Other interesting proteins found to be *S*-nitrosylated in the *Ljgsnor1* mutants are cysteine proteinase isoform 1, ubiquitin-conjugated enzyme and proteasome subunit beta type 1. All three are involved in protein degradation and linked to the senescence process. The *S*-nitrosylation of *S*-adenosylmethionine synthetase (SAMS) may be particularly important because this enzyme family participates in the biosynthetic pathways of ethylene, nicotianamine and polyamines, and provides the methyl group for protein and DNA methylation (Sauter et al. 2013). Specifically, the *A. thaliana* closest homolog to the SAMS isoform identified in this study is linked to ethylene synthesis (Mao et al. 2015). In rice (*Oryza sativa*) there are three SAMS isoforms implicated in the regulation of gene expression through their participation in methylation reactions. Down-regulation of the three genes caused dwarfism, reduced fertility, delayed germination and late flowering (Li et al. 2011). Finally, other proteins identified as preferentially *S*-nitrosylated targets in the mutants are related to photosynthesis and photorespiration, development, redox control and sulfur assimilation (**Table 2**).

Overall, our results suggest that increased *S*-nitrosylation of certain proteins that are essential for normal plant growth and development caused, at least to some extent, the phenotypes observed in the *Ljgsnor* mutants. Nevertheless, a number of limitations to this type of studies, based on the enrichment and identification of modified proteins, must be taken into consideration. While relatively abundant proteins are readily

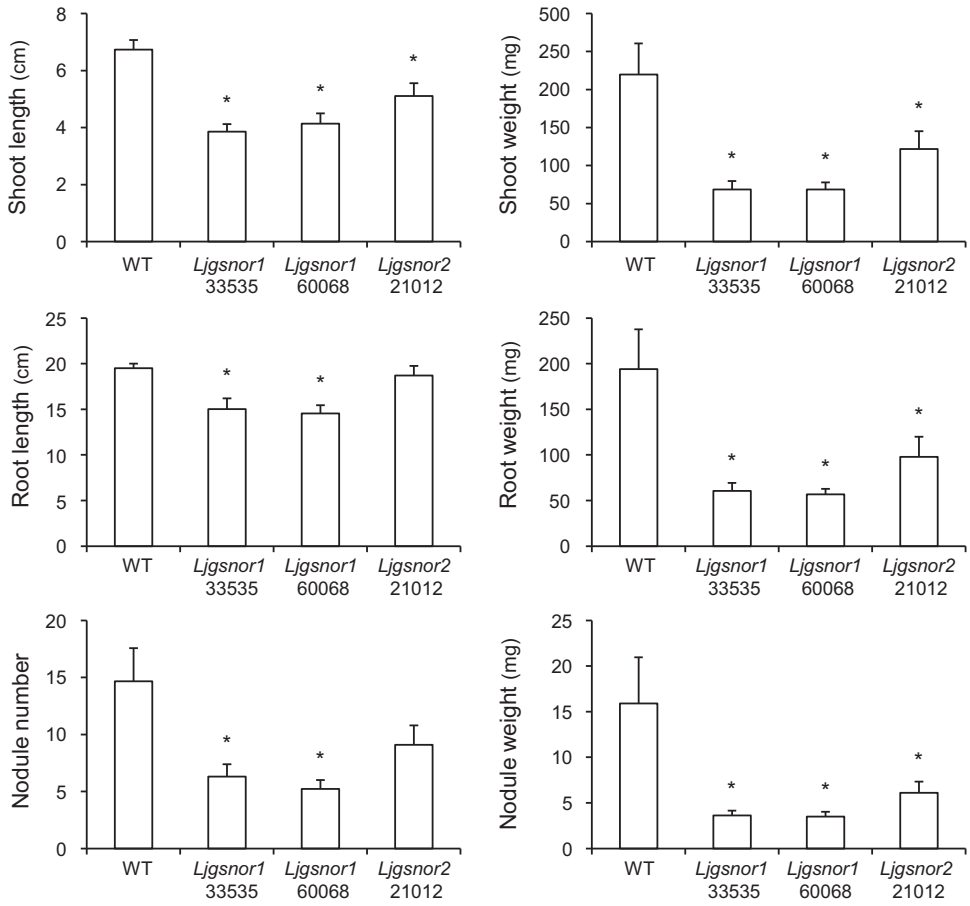

Fig. 7 Phenotypes of WT, *Ljgsnor1* and *Ljgsnor2* plants at 56 d of age. Seedlings were inoculated with *M. loti* strain R7A in plates containing Jensen medium and grown for 28 d in a controlled-environment chamber. The plants were then transferred to vermiculite-containing pots and grown for another 28 d. Values are means ± SE of 10–14 plants. Means marked with an asterisk differ significantly from control at *P*-value <0.05 based on the Student's *t*-test. The phenotyping was repeated three times with independently grown sets of plants with similar results.

identified as *S*-nitrosylated, low abundant but important signaling enzymes or transcription factors may be overlooked. Different degrees of *S*-nitrosylation or highly delimited spatio-temporal modifications are difficult to detect and might greatly influence plant development. Focused studies on specific pathways are therefore necessary. For instance, the morphological defects observed in the loss-of-function *Atgsnor1–3* mutant may result from perturbed signaling due to increased *S*-nitrosylation of key components required for auxin signaling and transport (Shi et al. 2015). In fact, AtGSNOR itself may be inhibited by *S*-nitrosylation elicited by NO derived from nitrate assimilation (Frungillo et al. 2014). These authors proposed a model in which increased GSNO levels feedback regulate nitrate uptake and reduction.

In summary, in this work two *GSNOR* genes have been identified and their protein products functionally characterized for the first time within the same plant species. The *LjGSNOR1* and *LjGSNOR2* genes show distinct expression profiles in tissues, but both enzymes have similar kinetics with respect to GSNO and hGSNO as substrates. The proteins are subjected to redox-dependent PTMs in vitro and in vivo, which strongly suggests that plant GSNORs may be important regulatory hubs by integrating signals mediated by H_2O_2, NO and H_2S. The *Ljgsnor1* and *Ljgsnor2* mutant plants have impaired nodule development and delayed formation of flowers and pods. The *Ljgsnor1* mutant contains 19 proteins that are specifically *S*-nitrosylated and are involved in defense and stress responses, protein degradation, hormone biosynthesis and photosynthesis. It is proposed that, in plants defective in GSNOR, *S*-nitrosylation of specific target proteins results in profound alterations of plant and nodule development.

Materials and Methods

Biological material

Plants of WT and mutant lines of *L. japonicus* ecotype Gifu B-129 were used in this study. The mutant lines were obtained from the *LORE1* collection (Małolepszy et al. 2016), with the following formal accession codes: lines 30033535 and 30060068 for Lj1g3v4528570 (knockouts for *LjGSNOR1*) and line 30021012 for Lj0g3v0071329 (knockout for *LjGSNOR2*). For simplicity, the lines are referred to as 33535, 60068 and 21012. Only one mutant line was selected for *LjGSNOR2* as it has only one exonic insertion and an additional intronic insertion (*Lotus* Base; **https://lotus.au.dk/**). Genotyping for selection of homozygous mutant plants was performed with PCR using primers for detection of *LORE1* insertions suggested from the *Lotus* Base. The PCR program was 94°C for 3 min, 40 cycles of 94°C for 15 s, 61°C for 15 s and 72°C for 40 s, with a final elongation step at 72°C for 7 min. Forward primers were used with

LORE1-specific primer P2 to detect *loci* with *LORE1* insertions. Reverse primers together with forward primers yield a PCR product only if the *locus* they flank does not contain an insertion (**Supplementary Table S1**).

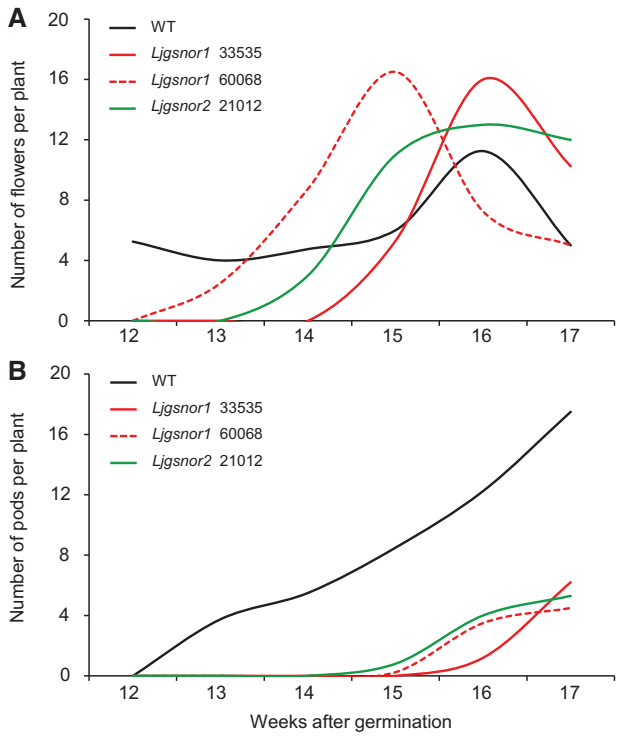

Fig. 8 Flowering (A) and fruiting (B) time-course of WT, *Ljgsnor1* and *Ljgsnor2* plants. Plants were grown in vermiculite-containing pots for 17 weeks. Values are means ± SE of 10–20 plants. The phenotyping was repeated twice with independently grown sets of plants with similar results.

Seeds from WT and homozygous mutant plants were scarified, sterilized, imbibed overnight at 25°C, synchronized for 2–3 d at 4°C on 0.5% (w/v) water agar plates and germinated for 3 d at 23°C in the dark. Seedlings were then transferred to 14 cm diameter plates containing Jensen medium (van Brussel et al. 1982), inoculated with *Mesorhizobium loti* strain R7A and grown in a controlled-environment chamber with a day/night regime of 23°C/21°C, 200 µmol $m^{-2}s^{-1}$ and 16 h photoperiod. After 28 d from germination, plants were phenotyped, transferred to 12.5 cm diameter pots containing vermiculite and watered twice a week with B&D nutrient solution (Broughton and Dilworth 1971) supplemented with 0.25 mM NH_4NO_3. Plants were phenotyped again at 56 d. Leaves, roots and nodules were harvested from 56 d-old-plants in liquid nitrogen and stored at −80°C. Flowers, pollen, pods, seeds and embryos were collected as described (Tovar-Méndez et al. 2011).

For hypocotyl elongation experiments, seeds were scarified, imbibed overnight at 25°C and synchronized for 2–3 d at 4°C on nutrient medium plates (Haughn and Somerville 1986) containing 0.5% (w/v) sucrose and 0.7% (w/v) agar. Seeds were germinated in the dark for 3 d in a growth chamber with a day/night regime of 23°C/21°C. After germination, the plates were placed vertically and the seedlings were allowed to grow in the dark for three additional days during which the increment of hypocotyl length was measured.

Expression analysis of *LjGSNOR* genes

Total RNA was extracted from nodules and processed as described (Ramos et al. 2009). qRT-PCR was performed using a 7500 Real-Time PCR System (Applied Biosystems, Waltham, MA, USA) with the primers listed in **Supplementary Table S1**. The primer efficiencies, calculated by serial dilutions of cDNAs, were in all cases >96%. Transcript levels were normalized using the geometric mean of two housekeeping genes, *ubiquitin* (DQ249171) and *ATP synthase* (AW719841).

Expression and purification of recombinant proteins

Gene sequences were obtained from the *Lotus* Base (Mun et al. 2016). The *LjGSNOR1* and *LjGSNOR2* open reading frames were inserted into *Nde*I and *Xho*I sites of the pET-30a(+) vector (Novagen, Merck, Darmstadt, Germany). Protein expression was induced in *E. coli* CD41 (DE3) cells by addition of 0.1 mM isopropyl-*β*-D-thiogalactopyranoside for 16 h at 20°C. Bacteria were harvested by centrifugation and resuspended in 50 mM potassium phosphate (pH 8.0) containing 10 mM $MgCl_2$, 300 mM NaCl, 40 mM imidazole, 20 mM

Table 2 Proteins identified as preferentially *S*-nitrosylated in *Ljgsnor1* mutant lines

Identifier	Protein	Functional category	*S*-NO prediction
Lj4g3v2775540.1	WD repeat domain-containing protein	Signaling	C198, C203, C234
Lj1g3v3330050.1	Chitinase (class Ia)	Biotic stress	C199
Lj5g3v2112210.1	Basic secretory protein	Biotic stress	C7
Lj3g3v0821380.1	Disease resistance response protein	Biotic stress	
Lj6g3v2156520.1	PSII reaction center psbP domain	Photosynthesis	C72
Lj3g3v3081260.1	Rubisco large subunit-binding protein	Photosynthesis	
Lj1g3v2842370.1	Phosphoglycolate phosphatase-like	Photorespiration	C19, C51
Lj0g3v0292899.2	GLABRA2 expression modulator	Development	C105
Lj1g3v4830650.1	*S*-adenosylmethionine synthetase	General function	C20
Lj6g3v0270780.1	Adenosylhomocysteinase	General function	
Lj4g3v0510180.1	Cysteine synthase	Amino acid metabolism	C12, C39
Lj5g3v0659730.2	Adenosine kinase 2-like	Nucleotide metabolism	
Lj4g3v2215040.1	Peroxiredoxin Q	Redox	C6, C62
Lj5g3v1697130.1	Chaperonin CPN60-like	Protein folding	C122, C244
Lj0g3v0355759.1	Ubiquitin-conjugating enzyme	Protein degradation	
Lj0g3v0162449.1	Cysteine proteinase 1-like	Protein degradation	C151, C299
Lj3g3v2735090.1	Proteasome subunit beta type-1-like	Protein degradation	C27
Lj4g3v1120500.1	Soluble inorganic pyrophosphatase	Miscellaneous	C15
Lj0g3v0339299.1	Quinone oxidoreductase-like protein	Miscellaneous	

Total proteins from leaf extracts were subjected to the biotin switch, affinity purified and identified by liquid chromatography–electrospray ionization–tandem MS. Only proteins detected in the two independent mutant lines, but not found in the WT, were chosen as robust candidates. *S*-nitrosylation sites were predicted using the GPS-SNO 1.0 software.

β-mercaptoethanol and 5% (v/v) glycerol. After sonication (6 × 30 s), extracts were cleared by centrifugation. The supernatants were loaded onto HiTrap chelating HP Ni-affinity columns (GE Healthcare Life Sciences) and the His-tagged proteins were eluted with buffer supplemented with 250 mM imidazole. Proteins were dialyzed overnight at 4°C in 25 mM Tris–HCl (pH 8.0) containing 20 mM β-mercaptoethanol and 5% (v/v) glycerol, and were concentrated by ultrafiltration. Protein was aliquoted, frozen in liquid nitrogen and stored at −80°C.

Biochemical assays

Recombinant LjGSNOR1 and LjGSNOR2 activities were determined by monitoring NADH oxidation using an extinction coefficient at 340 nm of 6.22 $mM^{-1}cm^{-1}$. The reaction mixture contained 25 mM Tris–HCl (pH 8.0), 0.2 mM NADH and 0.4 mM GSNO. Kinetic constants were determined for GSNO and hGSNO using concentrations ranging from 2.5 µM to 0.5 mM. Kinetic constants were also calculated for HMGSH using concentrations ranging from 20 µM to 1 mM. In this case, the enzymatic activity was determined following the formation of NADH at 340 nm in a reaction mixture composed of 25 mM Tris–HCl (pH 8.0), 2.5 mM NAD^+ and HMGSH.

GSNO and hGSNO were synthesized by mixing equal concentrations of GSH or hGSH and $NaNO_2$ dissolved in 0.25 M HCl/0.1 mM diethylenetriaminepentaacetic acid (DTPA). After 30 min incubation in darkness on ice with shaking, the reaction mixture was diluted 1:1 (v/v) with 50 mM sodium phosphate buffer (pH 7.4) and 75 µM NaOH. (h)GSNO concentration was determined using an extinction coefficient at 335 nm of 0.85 $mM^{-1}cm^{-1}$. HMGSH was synthesized by mixing equal volumes of GSH and formaldehyde in concentrations according to the equilibrium $K_{eq} = [HMGSH]/([GSH] - [HMGSH])([HCHO] - [HMGSH])$, where $K_{eq} = 1.77$ mM (Sanghani et al. 2000).

To investigate the effect of PTMs on enzyme activities, LjGSNOR1 and LjGSNOR2 were treated with 5 mM of several redox-active compounds: H_2O_2, DTT, β-mercaptoethanol, NaHS or GSNO for 1 h at 30°C in the dark. Excess reagents were removed by ultrafiltration and enzyme activity was assayed as described above. For glutathionylation assays, samples were incubated with 5 mM GSSG or 25 mM Tris–HCl (pH 8.0) for controls, for 5 h at 30°C. The molecular masses of LjGSNOR1 and LjGSNOR2 were determined before and after treatment with GSSG by MALDI-TOF MS with a 4800 Plus MALDI TOF/TOF analyzer (Sciex, Belgium). Briefly, proteins were acidified with 0.1% trifluoroacetic acid (TFA). Sample (0.5 µl) and matrix (0.5 µl of saturated solution of 10 mg ml^{-1} sinapinic acid prepared in 50% acetonitrile/0.1% TFA) were spotted onto an Opti-Tof 384-well insert (Sciex). MALDI-TOF MS analyses were performed in the linear mode with an accelerating voltage of 20 kV, mass range of 25–150 kDa, 1,000 shots/spectrum and laser intensity of 4,500. Spectra were externally calibrated with a standard protein mixture (ProteoMass Protein MALDI-MS Calibration Kit MSCAL3, Sigma, St Louis, MO, USA).

To determine GSNOR activity, leaves (∼100 mg) were homogeneized in 250 µl of buffer consisting of 50 mM Tris–HCl (pH 8.0), 2 mM DTT and Complete Mini EDTA-free Protease Inhibitor Cocktail (Roche, Basel, Switzerland). The supernatant was cleared by centrifugation (13,000×*g*, 10 min, 4°C) and desalted on NAP-5 columns (GE Healthcare), and the enzyme activity was determined as described for recombinant proteins.

SNO content

All steps were performed under dim light or darkness to avoid SNO losses due to the high sensitivity of the S-NO bond to light. Leaves (∼2 g) were harvested from 56 d-old plants, immediately ground to a fine powder in liquid nitrogen, and homogeneized in 2 ml of HEN buffer (100 mM HEPES, 0.1 mM DTPA, 0.01 mM neocuproine, pH 8.0). After two centrifugations (10,000×*g*, 10 min, 4°C), the samples were filtered through 0.22-µm membranes. To stabilize SNOs, free thiols were blocked with 10 mM *N*-ethylmaleimide for 15 min. Next, nitrite anions that could interfere with SNO measurement were eliminated by incubation with 10 mM of acidified sulfanilamide for 45 min on ice. The SNO content was determined with an NOA (Sievers, NOA-280i). For all samples, measurements were taken before and after incubation with 8.1 mM $HgCl_2$ for 30 min on ice. Hg^{2+} catalyzes the release of NO^+ from SNOs, causing a decrease in the NOA signal proportional to SNO concentration, which was calculated according to a standard curve with different GSNO concentrations.

Identification of *S*-nitrosylated proteins

Leaves from WT and *Ljgsnor1* mutant plants at 56 d of age were homogenized in HEN buffer. The extracts were centrifuged at 20,000×*g* and the supernatants diluted to 1 mg protein ml^{-1} in HEN buffer. Free thiols in the proteins (100 µg) were blocked with 100 mM *N*-ethylmaleimide in HEN buffer containing 2.5% SDS for 1 h at 37°C in the dark with shaking. Excess *N*-ethylmaleimide was removed by acetone precipitation/washing and proteins were solubilized in HENS buffer (HEN + 1% SDS). The biotin-switch assay (Jaffrey et al. 2001) was performed by incubation with 20 mM ascorbate and 0.25 mg ml^{-1} HPDP-Biotin (Pierce, Rockford, IL, USA) for 1 h at 37°C in the dark. Excess reagents were removed by acetone precipitation and washing. Dry pellets were resuspended in binding buffer consisting of 25 mM HEPES (pH 7.7), 1 mM EDTA, 100 mM NaCl, 0.8% Triton X-100 and 50 µl of streptavidin-agarose resin (Sigma). Samples were incubated for 16 h with occasional shaking at 4°C and then the agarose beads were washed ten times with a buffer comprising 25 mM HEPES (pH 7.7), 1 mM EDTA, 600 mM NaCl and 0.8% Triton X-100. Biotinylated proteins were eluted by incubating the beads in 50 mM HEPES (pH 7.7) and 100 mM DTT for 60 min at room temperature in the dark. Eluted proteins were digested with 0.5 µg of sequencing grade endoproteinase Lys-C (Roche) in 8 M urea for 5 h at 30°C. For trypsin digestion, samples were diluted 1:4 in trypsin buffer (10% acetonitrile, 50 mM NH_4HCO_3, 2 mM $CaCl_2$, 5 mM DTT), and proteins were digested with 1.5 µl of Poroszyme bulk immobilized trypsin beads (Applied Biosystems) at 37°C overnight. Digested proteins were desalted by solid-phase extraction using Oasis HLB cartridges (Waters, Milford, MA, USA). Peptides were eluted with methanol, vacuum dried and stored until use.

Liquid chromatography–electrospray ionization–tandem MS

Protein digests were re-dissolved in 2% acetonitrile and 0.1% formic acid, ultrasonicated for 15 s and centrifuged (10,000×*g*, 5 min, 4°C). An uHPLC system (Dionex Ultimate 3000, Thermo Fisher Scientific, Waltham, MA, USA) with a flow rate of 300 µl min^{-1} was used. The column (Thermo Scientific Easy Spray column) was loaded with <0.5 µg protein digest and the peptides were eluted with a 90-min gradient from 2% to 90% acetonitrile containing 0.1% formic acid. MS analysis was carried out with a Thermo Scientific Q Exactive Hybrid Quadrupole-Orbitrap mass spectrometer using a data-dependent top 20 method dynamically choosing the most abundant precursor ions from the survey scan (*m*/*z* 400–1,800 and a resolution of 70,000) for higher energy collisional dissociation fragmentation. Default charge state was set to 2-fold charge; unassigned charge states as well as +1 charge states were rejected. Minimal required signal was set to 10,000, size of exclusion mass list was set to 500 (with a duration of 60 s), and exclusion mass width was set to 4 ppm with one repeated count of 30 s.

Protein identification and mining

Analysis of mass spectral data was performed using MaxQuant (1.6.5.0). Raw files were searched against a FASTA file of the *Lotus* Base (Mun et al. 2016). Tryptic peptides were allowed a maximum of 2 missed cleavages as well as a maximum of three modifications per peptide (oxidation, N-terminal acetylation, *S*-nitrosylation). Precursor mass tolerance was set to 4.5 ppm (Fourier-Transform MS) and 0.6 Da (Ion Trap MS). To eliminate matching by chance, data was searched against a database of revert sequences in a target-decoy approach. Only high confidence peptides (false discovery rate < 0.01%), as well as proteins with at least two distinct identified peptides, passed the criteria for identification. Additionally, the false discovery rate based 'matching between runs' algorithm was used (Cox and Mann 2008). Proteins were functionally categorized on the basis of sequence similarity with proteins from other organisms via BLAST and RPS-BLAST against reference databases (ORYZA, PPAP, TAIR, KOG and CDD) using the Mercator sequence annotation tool (**http://plabipd.de/portal/mercator-sequence-annotation**; Lohse et al. 2014). Proteins that could not be assigned to specific bins by Mercator remained as 'not assigned'. For filtering putative *S*-nitrosylated proteins, major protein group ID lists were compared and those that were only detected in at least two replicates of the mutant lines, but not found in the WT, were selected as robust candidates.

Funding

Spanish Ministry of Economy and Competitiveness/State Research Agency-European Regional Developmental Fund [grant AGL2017-85775-R], Aragón Government (A09_17R) and Danish National Research Foundation [grant DNRF79].

Acknowledgments

We thank Carmen Pérez-Rontomé for valuable help with plant phenotyping and figure editing. The Proteomics Unit is a member of ProteoRed, Instituto de Salud Carlos III.

Disclosures

The authors have no conflicts of interest to declare.

References

Aroca, A., Gotor, C. and Romero, L.C. (2018) Hydrogen sulfide signaling in plants: emerging roles of protein persulfidation. *Front. Plant Sci.* 9: 1369.

Begara-Morales, J.C., Chaki, M., Valderrama, R., Sánchez-Calvo, B., Mata-Pérez, C., Padilla, M.N., et al. (2018) Nitric oxide buffering and conditional nitric oxide release in stress response. *J. Exp. Bot.* 69: 3425–3438.

Begara-Morales, J.C., Sánchez-Calvo, B., Chaki, M., Valderrama, R., Mata-Pérez, C., López-Jaramillo, J., et al. (2014) Dual regulation of cytosolic ascorbate peroxidase (APX) by tyrosine nitration and *S*-nitrosylation. *J Exp Bot.* 65: 527–538.

Benhar, M., Forrester, M.T., Hess, D.T. and Stamler, J.S. (2008) Regulated protein denitrosylation by cytosolic and mitochondrial thioredoxins. *Science* 320: 1050–1054.

Broughton, B.J. and Dilworth, M.J. (1971) Control of leghaemoglobin synthesis in snake beans. *Biochem. J.* 125: 1075–1080.

Camejo, D., Ortiz-Espín, A., Lázaro, J.J., Romero-Puertas, M.C., Lázaro-Payo, A., Sevilla, F., et al. (2015) Functional and structural changes in plant mitochondrial PrxII F caused by NO. *J. Proteomics* 119: 112–125.

Corpas, F.J., Alché, J.D. and Barroso, J.B. (2013) Current overview of *S*-nitrosoglutathione (GSNO) in higher plants. *Front. Plant Sci.* 4: 126.

Correa-Aragunde, N., Foresi, N., Delledonne, M. and Lamattina, L. (2013) Auxin induces redox regulation of ascorbate peroxidase 1 activity by *S*-nitrosylation/denitrosylation balance resulting in changes of root growth pattern in Arabidopsis. *J. Exp. Bot.* 64: 3339–3349.

Cox, J. and Mann, M. (2008) MaxQuant enables high peptide identification rates, individualized ppb-range mass accuracies and proteome-wide protein quantification. *Nat. Biotechnol.* 26: 1367–1372.

Díaz, M., Achkor, H., Titarenko, E. and Martínez, M.C. (2003) The gene encoding glutathione-dependent formaldehyde dehydrogenase/GSNO reductase is responsive to wounding, jasmonic acid and salicylic acid. *FEBS Lett.* 543: 136–139.

Domingos, P., Prado, A.M., Wong, A., Gehring, C. and Feijo, J.A. (2015) Nitric oxide: a multitasked signaling gas in plants. *Mol. Plant* 8: 506–520.

Feechan, A., Kwon, E., Yun, B.W., Wang, Y., Pallas, J.A. and Loake, G.J. (2005) A central role for *S*-nitrosothiols in plant disease resistance. *Proc. Natl. Acad. Sci. USA* 102: 8054–8059.

Frendo, P., Gallesi, D., Turnbull, R., Van de Sype, G., Hérouart, D. and Puppo, A. (1999) Localisation of glutathione and homoglutathione in *Medicago truncatula* is correlated to a differential expression of genes involved in their synthesis. *Plant J.* 17: 215–219.

Frendo, P., Matamoros, M.A., Alloing, G. and Becana, M. (2013) Thiol-based redox signaling in the nitrogen-fixing symbiosis. *Front. Plant Sci.* 4: 376.

Frungillo, L., Skelly, M.J., Loake, G.J., Spoel, S.H. and Salgado, I. (2014) *S*-nitrosothiols regulate nitric oxide production and storage in plants through the nitrogen assimilation pathway. *Nat. Commun.* 5: 5401.

Gong, B., Wen, D., Wang, X., Wei, M., Yang, F., Li, Y., et al. (2015) *S*-Nitrosoglutathione reductase-modulated redox signaling controls sodic alkaline stress responses in *Solanum lycopersicum* L. *Plant Cell Physiol.* 56: 790–802.

Gourion, B., Berrabah, F., Ratet, P. and Stacey, G. (2015) *Rhizobium*-legume symbioses: the crucial role of plant immunity. *Trends Plant Sci.* 20: 186–194.

Guerra, D., Ballard, K., Truebridge, I. and Vierling, E. (2016) *S*-Nitrosation of conserved cysteines modulates activity and stability of *S*-nitrosoglutathione reductase (GSNOR). *Biochemistry* 55: 2452–2464.

Haughn, G.W. and Somerville, C. (1986) Sulfonylurea-resistant mutants of *Arabidopsis thaliana*. *Molec. Gen. Genet.* 204: 430–434.

Hirst, D.G. and Robson, T. (2011) Nitric oxide physiology and pathology. *Methods Mol. Biol.* 704: 1–13.

Hu, J., Huang, X., Chen, L., Sun, X., Lu, C., Zhang, L., et al. (2015) Site-specific nitrosoproteomic identification of endogenously *S*-nitrosylated proteins in Arabidopsis. *Plant Physiol.* 167: 1731–1746.

Hussain, A., Yun, B.-W., Kim, J.H., Gupta, K.J., Hyung, N.-I. and Loake, G.J. (2019) Novel and conserved functions of *S*-nitrosoglutathione reductase in tomato. *J. Exp. Bot.* 70: 4877–4886.

Jaffrey, S.R., Erdjument-Bromage, H., Ferris, C.D., Tempst, P. and Snyder, S.H. (2001) Protein *S*-nitrosylation: a physiological signal for neuronal nitric oxide. *Nat. Cell Biol.* 3: 193–197.

Jensen, D.E., Belka, G.K. and Du Bois, G.C. (1998) *S*-nitrosoglutathione is a substrate for rat alcohol dehydrogenase class III isoenzyme. *Biochem. J.* 331: 659–668.

Kovacs, I. and Lindermayr, C. (2013) Nitric oxide-based protein modification: formation and site-specificity of protein *S*-nitrosylation. *Front. Plant Sci.* 4: 137.

Kovacs, I., Holzmeister, C., Wirtz, M., Geerlof, A., Fröhlich, T., Römling, G., et al. (2016) ROS-mediated inhibition of *S*-nitrosoglutathione reductase contributes to the activation of anti-oxidative mechanisms. *Front. Plant Sci.* 7: 1669.

Kubienová, L., Kopečný, D., Tylichová, M., Briozzo, P., Skopalová, J., Sebela, M., et al. (2013) Structural and functional characterization of a plant *S*-nitrosoglutathione reductase from *Solanum lycopersicum*. *Biochimie* 95: 889–902.

Kubienová, L., Tichá, T., Jahnová, J., Luhová, L., Mieslerová, B. and Petřivalský, M. (2014) Effect of abiotic stress stimuli on *S*-nitrosoglutathione reductase in plants. *Planta* 239: 139–146.

Kwon, E., Feechan, A., Yun, B.-W., Hwang, B.-H., Pallas, J.A., Kang, J.-G., et al. (2012) AtGSNOR1 function is required for multiple developmental programs in Arabidopsis. *Planta* 236: 887–900.

Lee, U., Wie, C., Fernández, B.O., Feelisch, M. and Vierling, E. (2008) Modulation of nitrosative stress by *S*-nitrosoglutathione reductase is critical for thermotolerance and plant growth in Arabidopsis. *Plant Cell* 20: 786–802.

Li, W., Han, Y., Tao, F. and Chong, K. (2011) Knockdown of SAMS genes encoding *S*-adenosyl-L-methionine synthetases causes methylation alterations of DNAs and histones and leads to late flowering in rice. *J. Plant Physiol.* 168: 1837–1843.

Lindermayr, C. (2018) Crosstalk between reactive oxygen species and nitric oxide in plants: key role of *S*-nitrosoglutathione reductase. *Free Radic. Biol. Med.* 122: 110–115.

Liu, L., Hausladen, A., Zeng, M., Que, L., Heitman, J. and Stamler, J.S. (2001) A metabolic enzyme for *S*-nitrosothiol conserved from bacteria to humans. *Nature* 410: 490–494.

Lohse, M., Nagel, A., Herter, T., May, P., Schroda, M., Zrenner, R., et al. (2014) Mercator: A fast and simple web server for genome scale functional annotation of plant sequence data. *Plant. Cell Environ.* 37: 1250–1258.

Małolepszy, A., Mun, T., Sandal, N., Gupta, V., Dubin, M., Urbański, D., et al. (2016) The *LORE1* insertion mutant resource. *Plant J.* 88: 306–317.

Mao, D., Yu, F., Li, J., Van de Poel, B., Tan, D., Li, J., et al. (2015) FERONIA receptor kinase interacts with *S*-adenosylmethionine synthetase and

suppresses *S*-adenosylmethionine production and ethylene biosynthesis in Arabidopsis. *Plant Cell Environ.* 38: 2566–2574.

Martínez, M.C., Achkor, H., Persson, B., Fernández, M.R., Shafqat, J., Farrés, J., et al. (1996) *Arabidopsis* formaldehyde dehydrogenase. Molecular properties of plant class III alcohol dehydrogenase provide further insights into the origins, structure and function of plant class P and liver class I dehydrogenases. *Eur. J. Biochem.* 241: 849–857.

Martínez-Medina, A., Pescador, L., Fernández, I., Rodríguez-Serrano, M., García, J.M., Romero-Puertas, M.C., et al. (2019) Nitric oxide and phytoglobin PHYTOGB1 are regulatory elements in the *Solanum lycopersicum-Rhizophagus irregularis* mycorrhizal symbiosis. *New Phytol.* 223: 1560–1574.

Matamoros, M.A., Clemente, M.R., Sato, S., Asamizu, E., Tabata, S., Ramos, J., et al. (2003) Molecular analysis of the pathway for the synthesis of thiol tripeptides in the model legume *Lotus japonicus*. *Mol. Plant Microbe Interact.* 16: 1039–1046.

Matamoros, M.A., Moran, J.F., Iturbe-Ormaetxe, I., Rubio, M.C. and Becana, M. (1999) Glutathione and homoglutathione synthesis in legume root nodules. *Plant Physiol.* 121: 879–888.

Melchers, J., Dirdjaja, N., Ruppert, T. and Krauth-Siegel, R.L. (2007) Glutathionylation of trypanosomal thiol redox proteins. *J. Biol. Chem.* 282: 8678–8694.

Michelet, L., Zaffagnini, M., Marchand, C., Collin, V., Decottignies, P., Tsan, P., et al. (2005) Glutathionylation of chloroplast thioredoxin *f* is a redox signaling mechanism in plants. *Proc. Natl. Acad. Sci. USA* 102: 16478–16483.

Mun, T., Bachmann, A., Gupta, V., Stougaard, J. and Andersen, S.U. (2016) *Lotus* Base: an integrated information portal for the model legume *Lotus japonicus*. *Sci. Rep.* 6: 39447.

Noctor, G., Mhamdi, A., Chaouch, S., Han, Y., Neukermans, J., Márquez-García, B., et al. (2012) Glutathione in plants: an integrated overview. *Plant Cell Environ.* 35: 454–484.

Ono, K., Akaike, T., Sawa, T., Kumagai, Y., Wink, D.A., Tantillo, D.J., et al. (2014) Redox chemistry and chemical biology of H_2S, hydropersulfides, and derived species: implications of their possible biological activity and utility. *Free Radic. Biol. Med.* 77: 82–194.

Palmieri, M.C., Lindermayr, C., Bauwe, H., Steinhauser, C. and Durner, J. (2010) Regulation of plant glycine decarboxylase by *S*-nitrosylation and glutathionylation. *Plant Physiol.* 152: 1514–1528.

Ramos, J., Matamoros, M.A., Naya, L., James, E.K., Rouhier, N., Sato, S., et al. (2009) The glutathione peroxidase gene family of *Lotus japonicus*: characterization of genomic clones, expression analyses and immunolocalization in legumes. *New Phytol.* 181: 103–114.

Rieu, I. and Powers, S.J. (2009) Real-time quantitative RT-PCR: design, calculations, and statistics. *Plant Cell* 21: 1031–1033.

Rodríguez-Ruiz, M., Mateos, R.M., Codesido, V., Corpas, F.J. and Palma, J.M. (2017) Characterization of the galactono-1, 4-lactone dehydrogenase from pepper fruits and its modulation in the ascorbate biosynthesis. Role of nitric oxide. *Redox Biol.* 12: 171–181.

Romero-Puertas, M.C., Laxa, M., Matte, A., Zaninotto, F., Finkemeier, I., Jones, A.M., et al. (2007) *S*-nitrosylation of peroxiredoxin II E promotes peroxynitrite-mediated tyrosine nitration. *Plant Cell* 19: 4120–4130.

Rustérucci, C., Espunya, M.C., Díaz, M., Chabannes, M. and Martínez, M.C. (2007) *S*-nitrosoglutathione reductase affords protection against pathogens in Arabidopsis, both locally and systemically. *Plant Physiol.* 143: 1282–1292.

Sakamoto, A., Ueda, M. and Morikawa, H. (2002) Arabidopsis glutathione-dependent formaldehyde dehydrogenase is an *S*-nitrosoglutathione reductase. *FEBS Lett.* 515: 20–24.

Sanghani, P.C., Stone, C.L., Ray, B.D., Pindel, E.V., Hurley, T.D. and Bosron, W. F. (2000) Kinetic mechanism of human glutathione-dependent formaldehyde dehydrogenase. *Biochemistry* 39: 10720–10729.

Sato, S., Nakamura, Y., Kaneko, T., Asamizu, E., Kato, T., Nakao, M., et al. (2008) Genome structure of the legume, *Lotus japonicus*. *DNA Res.* 15: 227–239.

Sauter, M., Moffatt, B., Saechao, M.C., Hell, R. and Wirtz, M. (2013) Methionine salvage and *S*-adenosylmethionine: essential links between sulfur, ethylene and polyamine biosynthesis. *Biochem. J.* 451: 145–154.

Shi, Y.F., Wang, D.L., Wang, C., Culler, A.H., Kreiser, M.A., Suresh, J., et al. (2015) Loss of GSNOR1 function leads to compromised auxin signaling and polar auxin transport. *Mol. Plant* 8: 350–1365.

Tang, H., Krishnakumar, V., Bidwell, S., Rosen, B., Chan, A., Zhou, S., et al. (2014) An improved genome release (version Mt4.0) for the model legume *Medicago truncatula*. *BMC Genomics* 15: 312.

Tovar-Méndez, A., Matamoros, M.A., Bustos-Sanmamed, P., Dietz, K.J., Cejudo, F.J., Rouhier, N., et al. (2011) Peroxiredoxins and NADPH-dependent thioredoxin systems in the model legume *Lotus japonicus*. *Plant Physiol.* 156: 1535–1547.

Udvardi, M. and Poole, P.S. (2013) Transport and metabolism in legume-rhizobia symbioses. *Annu. Rev. Plant Biol.* 64: 781–805.

Umbreen, S., Lubega, J., Cui, B., Pan, Q., Jiang, J. and Loake, G.J. (2018) Specificity in nitric oxide signaling. *J. Exp. Bot.* 69: 3439–3448.

van Brussel, A.A.N., Tak, T., Wetselaar, A., Pees, E. and Wijffelman, C.A. (1982) Small leguminosae as test plants for nodulation of *Rhizobium leguminosarum* and other rhizobia and agrobacteria harbouring a leguminosarum Sym-plasmid. *Plant Sci. Lett.* 27: 317–325.

Xu, S., Guerra, D., Lee, U. and Vierling, E. (2013) *S*-nitrosoglutathione reductases are low copy number, cysteine-rich proteins in plants that control multiple developmental and defense responses in Arabidopsis. *Front. Plant Sci.* 4: 430.

Xue, Y., Liu, Z., Gao, X., Jin, C., Wen, L., Yao, X., et al. (2010) GPS-SNO: computational prediction of protein S-nitrosylation sites with a modified GPS algorithm. *PLoS One* 5: e11290.

Waszczak, C., Akter, S., Jacques, S., Huang, J., Messens, J. and Van Breusegem, F. (2015) Oxidative post-translational modifications of cysteine residues in plant signal transduction. *J. Exp. Bot.* 66: 2923–2934.

Winter, D., Vinegar, B., Nahal, H., Ammar, R., Wilson, G.V. and Provart, N.J. (2007) An "Electronic Fluorescent Pictograph" browser for exploring and analyzing large-scale biological data sets. *PLoS One* 2: e718.

Zaffagnini, M., Bedhomme, M., Lemaire, S.D. and Trost, P. (2012) The emerging roles of protein glutathionylation in chloroplasts. *Plant Sci.* 185–186: 86–96.

Zhang, J., Ye, Z.W., Singh, S., Townsend, D.M. and Tew, K.D. (2018) An evolving understanding of the *S*-glutathionylation cycle in pathways of redox regulation. *Free Radic. Biol. Med.* 120: 204–216.

Zechmann, B. (2014) Compartment-specific importance of glutathione during abiotic and biotic stress. *Front. Plant Sci.* 5: 566.